Zeitschrift: Helvetica Physica Acta
Band: 55 (1982)
Heft: 6

Artikel: Unsteady He^4 convection and related quantum constraints
Autor: Frederking, T.H.K.
DOI: https://doi.org/10.5169/seals-115307

Helvetica Physica Acta, Vol. 55 (1982) 711–719 0018–0238/82/060711–09$1.50 + 0.20/0

Unsteady He^4 convection and related quantum constraints

By T. H. K. Frederking, Walther-Meissner Institut,[1])
D-8046 Garching, Federal Republic of Germany[2])

(22. XII. 1982)

Abstract. In the course of transient stability studies of He II-cooled NbTi/Cu localized Benard convection may be observed in a He I layer above the lambda temperature. In this context quantization conditions are studied for the Newtonian fluid He I involving Onsager-Feynman vortices with quantized circulation. Stability data obtained support evolution of He I layer convection from cellular order toward turbulent disorder ('catastrophe'). Onset data support a vortex number of unity per cell consistent with minimum expenditure rates.

Introduction

In He II-cooled magnets, a loss of stability of NbTi/Cu below the lambda temperature (T_λ) brings about local heating beyond T_λ. In this context convection evolution is studied during transient operation with emphasis on vortex systems carrying quantized circulation. In particular the question of convection onset phenomena is examined whose minimum energy expenditure rate is obtained for one Onsager vortex per cell during ordered convection in Newtonian fluid. It is noted that so far quantum phenomena have found attention primarily in superfluid non-Newtonian systems. In the present study however, Newtonian fluid data have been obtained and compared with a convection model during evolution of flow patterns from ordered motion toward the catastrophe of turbulence. The few data available for onset of cellular convection indicate support for a quantum vortex number of unit per cell.

Convection model

The transport case considered as reference situation for the present transient experiments is cellular convection in a two-plate Rayleigh–Bénard [1] apparatus (Fig. 1). At Ra-numbers one order above Ra_c, flow modeling is based on the two-dimensional set of thermo-hydrodynamic equations (2)–(6):
Continuity:

$$\partial v_x/\partial x + \partial v_y/\partial y = 0 \qquad (1)$$

---

[1]) Zentralinstitut für Tieftemperaturforschung.
[2]) Permanent address: Univ. Calif. Los Angeles 90024 CA.

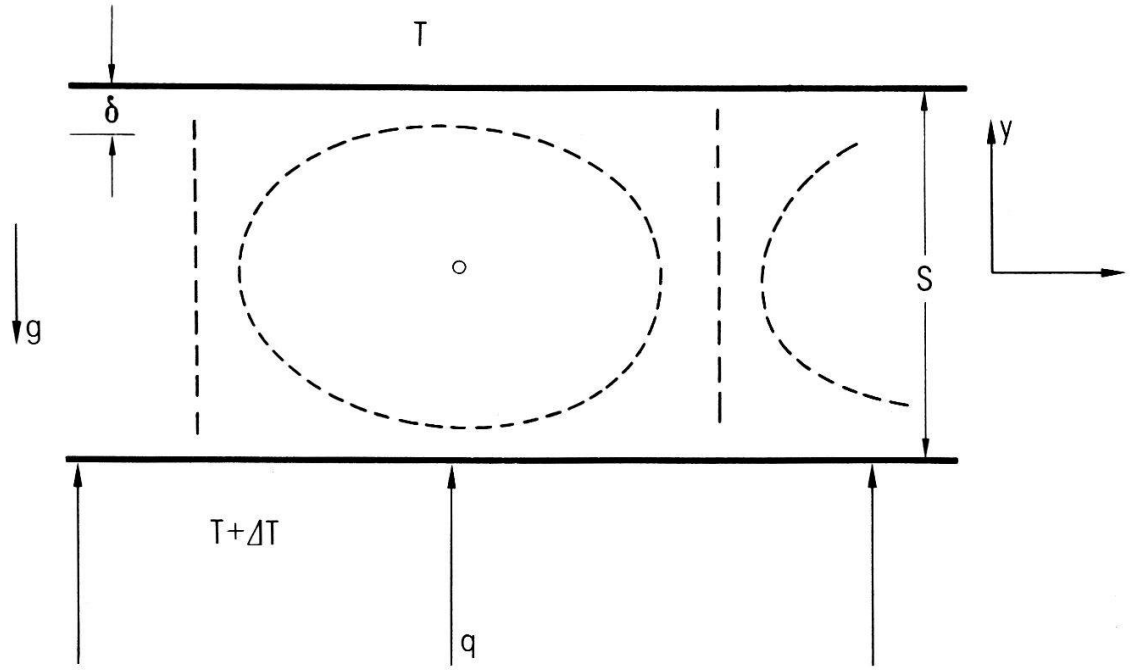

Figure 1
Simplified cellular convection pattern between Bénard plates: Lower plate heated, upper plate cooled.

Motion:

$$\rho\{v_x\,\partial v_x/\partial x + v_y\,\partial v_x/\partial y\} = g\rho\beta\theta + \eta\,\partial^2 v_x/\partial y^2 \tag{2}$$

Thermal energy convection:

$$\rho c_p v_x\,\partial\theta/\partial x = k\,\partial^2\theta/\partial y^2 \tag{3}$$

(x, y coordinates, v_x and v_y velocity components along the two axis). Boussinesq fluid is assumed with density changes ($\Delta\rho$) considered only in the buoyancy term $g\,\Delta\rho/\rho = \beta\,\Delta T g$ for $\Delta T \ll T$, (β isobaric expansivity, g gravitational acceleration). The local thermal energy density is ($\rho c_p\theta$), (c_p specific heat at constant pressure, θ local excess temperature, η shear viscosity, k thermal conductivity, Pr Prandtl number $\eta c_p/k$, $Ra = \mathrm{Pr}\,(s^3\rho^2 g\beta\,\Delta T/\eta^2)$, s plate spacing, Fig. 1). At the critical $\Delta T_c = \Delta T_c(Ra_c)$, heat diffusion ceases and convection is initiated ($Ra_c \sim 10^3$). After a transition, a cellular flow is established. The simplified cell system adopted has two cell domains: A central cell region of inviscid Euler fluid and viscous layers at each wall. The latter are attached on one side to the solid wall. On the other side they contact the Euler fluid. Newtonian fluid boundary conditions at the walls are $v_x = v_y = 0$. At the lower plate of the Bénard geometry we have $(T+\Delta T)$, and T at the upper plate. For this flow model the pertinent results may be written down [5]:
Dominant frequency (order of magnitude):

$$f \sim 0.1(k/s^2)(\rho c_p)^{-1} Ra^{1/2} \tag{4}$$

Characteristic speed of boundary layer fluid:

$$v_c \sim 0.1\{sg\beta\,\Delta T k/(\eta c_p)\}^{1/2} \tag{5}$$

Boundary layer thickness:

$$\delta \sim \{(s\eta k)/(g\rho^2\beta\,\Delta T c_p)\}^{1/4} \tag{6}$$

For instance, the upper dominant frequency reported by Gollub and Benson [7] is described by

$$(f/f_{\text{ref}}) = \zeta_L Ra^{1/2} \tag{7}$$

with a constant $\zeta_L = 0.13$ in the range of their data. The reference frequency is $f_{\text{ref}} = ks^{-2}/(\rho c_p)$. As Ra is increased, the flow kinematics is characterized by appearance of an additional set of frequencies [8]. Finally turbulence broadens the power spectrum. On dimensional grounds the lack of a size effect leads to the frequency condition:

$$(f/f_{\text{ref}}) = \zeta_{TB} Ra^{2/3} \tag{8a}$$

The coefficient ζ_{TB} describes the *order* of magnitude of the significant spectral range with turbulent disorder. Explicitly we have

$$f = \zeta_{TB} k(\rho c_p)^{-1}\{\rho^2\beta\,\Delta T c_p g/(\eta k)\}^{2/3} \tag{8b}$$

The frequency results compiled by Krishnamurti [9] as $\tau_c = f^{-1}$, show $\tau \sim Ra^{-2/3}$ in support of (8) with an order $\zeta_{TB} \sim 10^2$.

Convection onset

The preceding model does not describe initiation of convection. Therefore corrections may be applied, and it appears to be tempting to make use of the following functions: Frequency $f \sim (Ra - Ra_c)^{1/2}$, boundary layer thickness $\delta \sim (Ra - Ra_c)^{-1/4}$, (and similar functions). However, the thickness δ cannot grow beyond the half-spacing $(s/2)$ of the Bénard plates. Thus, at Ra_c we have $\delta \to (s/2)$. Mode calculations for this Ra-region $Ra \gtrapprox Ra_c$ lead to a linear function between $(Ra - Ra_c)$ and the increment in the dimensionless thermal energy transfer rate (Nusselt number $\text{Nu} \sim s/\delta$). This rate is governed by

$$\delta/s \approx \tfrac{1}{2}\{1 + \zeta_0(Ra - Ra_c)/Ra_c\}^{-1} \tag{9}$$

with a constant $\zeta_0 = 1.44$, [10]. At the convection onset the velocity $v_c = v_{cc}$ is associated with the kinetic energy, per unit volume, of $(\rho v_{cc}^2/2)$. This energy arises from the availability of potential energy, per unit volume, in the form of gravitational buoyancy at $\Delta T_c = \Delta T(Ra_c)$. The latter may be expressed as $|\nabla P_{\text{eff}}| \cdot s = g\beta\,|\Delta T|\,\rho s$. The resulting speed v_{cc} is proportional to $(gs\beta\,\Delta T_c)^{1/2}$, i.e. it is finite at Ra_c, as all governing quantities are finite. Once motion is established, for constant $\Delta T > T_c$, the quasi-steady system's mean speed remains finite due to viscous forces. Viscosity gives rise to dissipation of energy at a volumetric rate $\eta(\partial v_x/\partial y)^2$. In the time $\tau_c = \tau(Ra_c)$ the energy dissipated is calculated as $(\sim 0.1\,|\nabla P_{\text{eff}}|\,\tau_c/\eta)$. We have τ_c of the order $(s\pi/v_{cc})$. As v_{cc} remains finite, the characteristic time $\tau_c = f_c^{-1}$ also stays at a finite value. Thus, in contrast to the extended power law expressions quoted above, the dominant frequency $f_c = f(Ra_c)$ does not disappear. We obtain

$$\tau_c = f_c^{-1} \sim 10^2 \quad (\eta/\rho)/(sg\beta\,\Delta T)_c \tag{10}$$

Quantization constraints

Because of chaos during turbulent convection, the regime of very high Ra appears to be unaccessible to detailed quantum diagnosis. However cellular flow and onset of motion are characterized by well-defined model quantities discussed above. According to the Onsager–Feynman postulate of the existence of quantized vortices, the circulation around the center of the cell is a multiple of the quantum of circulation $\Gamma_0 = \hbar 2\pi/m$, ($\hbar$ Planck's quantum divided by 2π, m mass of the fluid's molecule):

$$\oint \vec{v} \cdot d\vec{l} = N_v \Gamma_0 = \Gamma \tag{11}$$

Making use of equations (5) and (6) we obtain a number of quantized vortices of

$$N_v \sim K(c_p \rho)^{-1} Ra^{1/2}/\Gamma_0 \tag{12}$$

For instance, for low temperature He^4 (= He I) the quantum of circulation is $\Gamma_0 = 10^{-3}$ cm^2/s. At 4 K and atmospheric pressure, for $Ra \sim 10Ra_c$, a number N_v between the order 10 and 10^2 results for the center vortex system of the cell. This order estimate presumes that no secondary vortices have been formed.

In contrast to the large numbers N_v of the cellular convection at $10Ra_c$, low finite numbers are expected at Ra_c. A minimum threshold value of $N_v = 1$ appears to comply with the lowest entropy rejection rate resulting from least action postulates. Thus, quantum constraints associate physical conditions with the details of the cell center discussed above.

Experiments

In the experiments a slab formed by a set of three composite conductors NbTi/Cu is used as 'conductor-in-box' configuration. A vacuum-insulated chamber (Fig. 2) acting as 'box' houses the horizontal slab. For thermal equilibration a duct is located above an upper hole in the cylindrical box. This vacuum-insulated tube carries turbulent Gorter–Mellink convection in case of *steady* heat transport in the q-range covered. The individual conductor sections have a length of $L_s = 2.54$ cm (overall) and approximately square cross section with base $a = 0.224$ cm. The inner diameter of the upper duct is $D_G = 0.605$ cm, and the box diameter is $D_B = 5.715$ cm (O.D.). The axial length has the value $L_v = 3.8$ cm. Heater sections are located inside the two outer conductors, and a carbon thermometer is installed in the central section of the slab. The set is connected by soldering at its lateral inner faces.

A step input in power is applied externally to the heater sections. As a result, the composite temperature is changed and recorded as thermometer signal $T(t)$. Saturated liquid He^4 serves as coolant. Further, for better stability the box liquid as well as an outer bath is kept below the lambda temperature prior to heat supply inside the box. At $t = 0$, application of the step input in power, $q > 0$, changes thermal conditions in the box. The composite conductor undergoes heating, reaches a relative maximum of $T = T_{max}$, and a subsequent relative minimum $T = T_{min}$, and attains a steady value (Fig. 3, insert). In the q-range

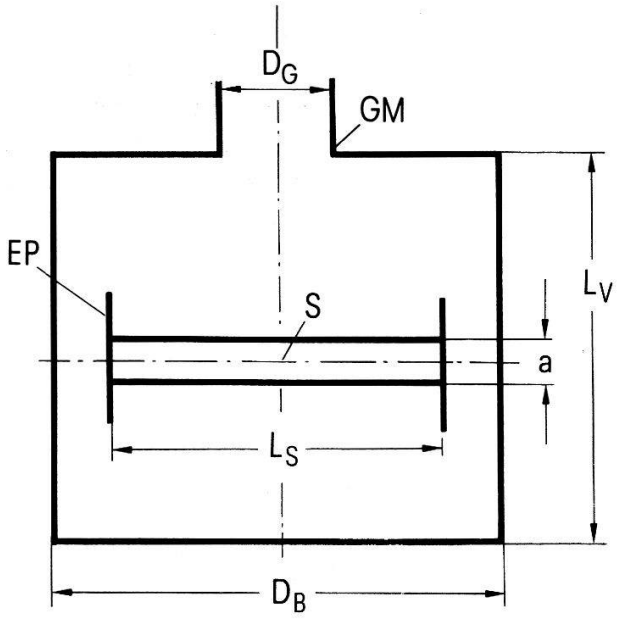

Figure 2
Vacuum-insulated 'conductor-in-box' system (schematically); *S* specimen NbTi/Cu; EP end plate (on both ends of the NbTi/Cu); GM opening with Gorter–Mellink duct.

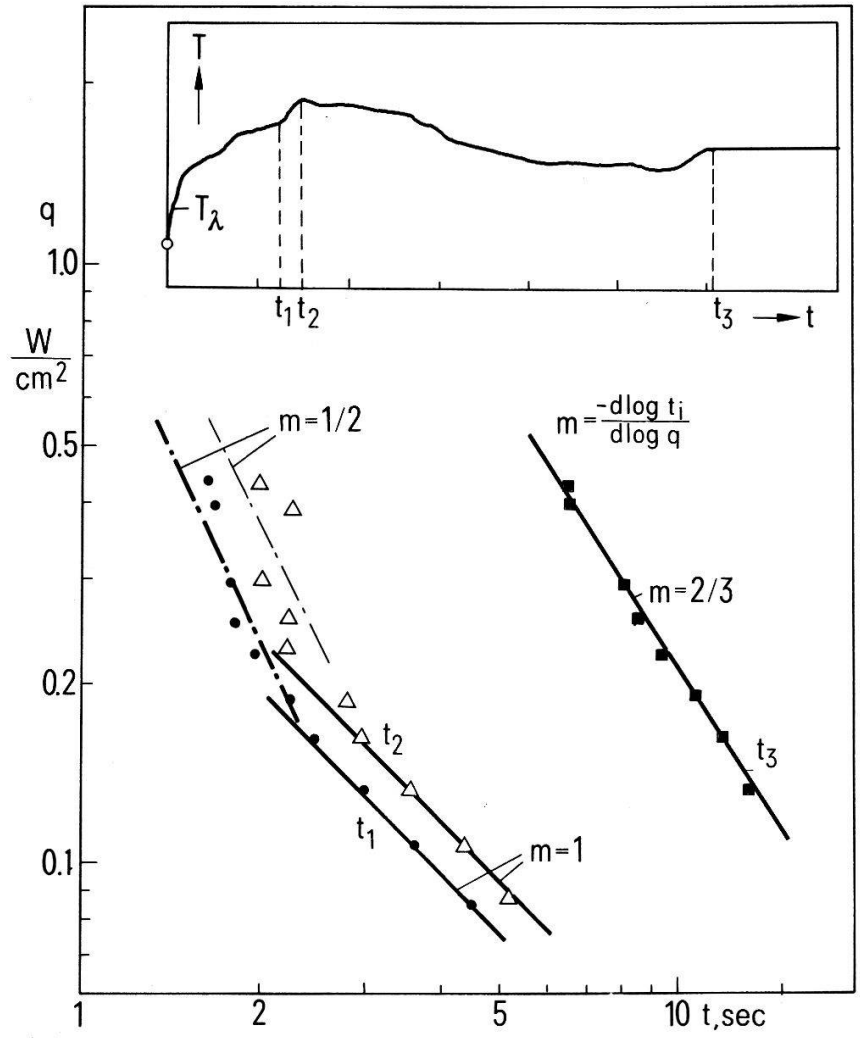

Figure 3
Step inputs at three different times t_i $(i = 1, 2, 3)$ marking a distinct change in the derivative dT/dt; Bulk fluid state: Saturated liquid He^4, bath temperature 2.05 K); Insert: Temperature of the NbTi/Cu as non-linear thermometer signal vs. time with t_i.

covered, discrete times (t_i) mark the occurrence of various events ($i = 1, 2, 3$ in Fig. 3). At t_1, a relatively drastic change in (dT/dt) is visible during the initial warmup interval. The maximum is characterized by $t(T_{max}) = t_2$. At the time t_3, T reaches its final value. In a limited range of q, the functions $q(t_i)$ are seen to be described by power laws (Fig. 3). Other details of various experiments at higher pressures, including the range above the thermodynamic critical pressure, have been described elsewhere [11].

Results and Discussion

In general the imposed heat flux density q is a monotonically decreasing function of time. This behavior is characterized by power laws with an exponent $m = -d \log t_i / d \log q$ of the order unity.

Times t_1. Thermal energy rejection rates at long times t_1, and small q, are in agreement with order of magnitude of $\Delta T \sim 0.01$ K. This order is derived from Gorter–Mellink convection details including the occurrence of local vapor cavity formation and subsequent T-redistribution. The composite conductor at t_1 is above the lambda temperature of 2.17 K. In contrast, bulk He^4 stays below this higher order phase transition temperature. At short times m is roughly (1/2). This value is consistent with the cellular convection, equation (7). As q is high, convection is localized in a wall-adjacent He I domain 'coating' the composite. The He I constitutes a thermal resistance between the solid-fluid interface and the He II in the box. The existence of localized Bénard convection in a very thin layer is accessible also from additional t_i-information.

Times t_2. The time interval t_2 needed to reach T_{max} is quite close to t_1. Figure 3 shows that the function $t_2(q)$ is very similar to $t_1(q)$. This indicates similarity also in the fluid convection patterns. For a specified q-value, the times t_1 are about 80% of the times t_2. As the overall Kapitza resistance governs the composite temperature (including the He I layer), there are related increases in the total ΔT-values from t_1 to t_2.

Times t_3. At the time t_3, the composite temperatute has reached the end of the second warm-up period after T_{min}. At t_3, the composite remains at the final steady value within thermometer resolution. The function $t_3(q)$ is characterized by the power exponent $m = 2/3$. To first order, the evidence obtained indicates an approximately constant He I thickness, and related ΔT_I-value of the He I-domain. The case $q = \text{const}$ has been described by a modified Ra-number [12] of the form $\widetilde{Ra} = \widetilde{Ra}\{qs/(k \cdot \Delta T_r)\}$. Thus, for the He I-conditions quoted, the $t_3(q)$-function appears to be closely related to equations (8) and (9). Accordingly, locally homogeneous turbulence appears to be established.

In principle, very thin He I layers do not exist as isolated resistances in the present transport. They interact with He I in the 'conductor-in-box' system. In spite of this complexity, transport analysis is facilitated by using the postulate of *local* thermodynamic equilibrium for the long times needed for t_i-events. This permits utilization of the phase transitions encountered [11] as additional tools for convection diagnosis. Further, we view the present convection evidence in the light of supplementary data sets for single-phase convection transients reported in Ref. 12. The results pertain to step inputs in power at high dimensionless times for low values of the difference $(\widetilde{Ra} - \widetilde{Ra}_c)$.

Quantum vortex system evidence

The number of quantized vortices of the cell core reaches a minimum value for $Ra \to Ra_c$ according to the preceding model constraints. As v_c decreases toward v_{cc}, however the time increases toward the large value τ_c. Observations appear to be limited, and values of the dimensionless time (τ/τ_{ref}) do not reach beyond 10 in Ref. 12; (The reference time is $\tau_{ref} = 1/f_{ref} = [\rho c_p s^2/k]$, [12]). The number of quantized cell vortices $N_v \to N_0$ is obtained for $\tau \to \tau_0$ from $\Gamma \sim (sv_{cc})$ and from condition (11): $[s^2\pi/\tau_0] \sim (N_0\Gamma_0)$. This leads to a minimum number of observed vortices

$$N_0 \approx \pi s^2/(\tau_0\Gamma_0) \tag{13}$$

The data for a fluid of molecular mass M are related to the present He^4-liquid by means of the ratio $(M/M_4) = (m/m_{He^4})$, (Reference case He^4 characterized by the subscript 4). N_0 is rewritten in terms of this ratio, and in terms of the observation limit (τ_0/τ_{ref}) [12]

$$N_0 \approx \pi(\tau_0/\tau_{ref})^{-1}(M/M_4)[k/(\rho c_p(\Gamma_0)_4)] \tag{14}$$

From the data of Ref. 12 a vortex number of the order 10 is obtained at the observation limit. Despite this high value, N_0 appears to be a reasonable upper bound, in particular in view of the limited experimental evidence. The departure of experimental Ra-data from Ra_c at the observation limit is specified [12] by $0 < (Ra - Ra_c) < 0.2$. Reference 4 suggests $N_v \sim 1$.

Model extension to He II

In superfluid He II quantum phenomena involving generation of vortices with $(\Gamma_0)_4$ are exhibited on a macroscopic scale. Using two-fluid concepts one may formulate restricted convection analogs in the asymptotic limit of 'pseudo-classical' convection [13] for very small roton concentrations. In this case, the superfluid density ratio is near unity and does not appear explicitly in the continuum equation adopted (Appendix A). For the two-plate Bénard apparatus, no prescribed orientation is needed because of the thermomechanical driving force. The Bénard analog of the model convection considered in Appendix A is obtained readily using the assumption of Newtonian behavior of the roton excitation system considered a normal fluid continuum. No detailed comparision with data appears to be possible as only a few experimental attempts have been made in this area.

Conclusions concerning quantum vortices are very limited in view of the scarce experimental evidence. Classical Newtonian fluid convection in the Bénard system indicates a low number of quantized cell vortices at the observation limit of convection onset. So far, the findings appear to be compatible with N_v of unity, expected for minimization of energy expenditure rates.

As to thermal boundary conditions of quenches of NbTi, the present data for localized He I domains indicate evolution of convection patterns during transients caused by a quench. The system undergoes a change from a low number of vortices toward a final state of locally homogeneous turbulence with a power law exponent $m = (2/3)$.

Acknowledgements

The experiments have been supported in part by NSF. I am most grateful to Professor K. Andres and to Walther–Meissner Institut for their support during the writing of this paper.

REFERENCES

[1] H. BÉNARD, Ann. Chem. Phys. *23*, 62 (1901).
[2] S. CHANDRASEKHAR, *Hydrodynamic and Hydromagnetic Stability*, Oxford, Univ. Press, Oxford 1961.
[3] F. H. BUSSE, *Transition to Turbulence in Rayleigh-Bénard Convection*, in *Hydrodyn. Instabilities and the Transition to Turbulence.* (Eds. H. L. Swinney and J. P. Gollub), Springer, Berlin 1981, p. 97.
[4] G. AHLERS, Phys. Rev. Letters. *33*, 1185 (1974).
[5] Y. KAMIOKA, C. CHUANG and T. H. K. FREDERKING, Refrig. Sci. Technology, Vol. 1, 1980; (IIR), p. 311.
[6] L. D. LANDAU and E. M. LIFSCHITZ, *Fluid Mechanics*, Pergamon, London 1959.
[7] J. P. GOLLUB and S. V. BENSON Phys. Rev. Letters *41*, 948 (1978).
[8] A. LIBCHABER, Physica 109 & 110B, 1583, 1982; J. MAURER and A. LIBCHABER, J. Phys. (Paris) *40*, 419 (1979).
[9] R. KRISHNAMURTI, J. Fluid Mech. *42*, 309 (1970).
[10] K. G. T. HOLLANDS, Phys. Fluids *8*, 389 (1965); I. CATTON, Phys. Fluids *9*, 2521 (1966).
[11]. C. CHUANG, Y. KAMIOKA and T. H. K. FREDERKING, Adv. Cryog. Eng. *27*, 493 (1982); C. CHUANG and T. H. K. FREDERKING, Cryogenics *22*, 423 (1982).
[12] R. C. NIELSEN and R. H. SABERSKY, Int. J. Heat Mass Transf. *16*, 2407 (1973).
[13] T. H. K. FREDERKING, Adv. Cryog. Eng. *27*, 399 (1982).

Appendix A. Pseudo-classical convection in He II in the roton depletion limit

Consider He II between Bénard plates with spacing s and fluid kept at $(T+\Delta T)$ on the heat side, and at T on the other side where thermal energy is removed. The fluid, assumed to be a Newtonian system representation of the excitations in superfluid He II, is 'pseudo classical' [13] with the following properties: {1}, Newtonian shear stress behavior; {2}. Nearly fully established order parameter with a super-fluid density ratio close to unity in the limit of depletion of rotational excitations (rotons); {3} Dominant convection cause is the thermo-osmotic (thermomechanical) gradient $\nabla P_{\text{eff}} = \rho S_L \nabla T$; {4}, Effective Prandtl number of unity (S_L entropy per unit mass of liquid). The two-dimensional equations of this pseudo-classical model fluid are the analog of equations (1) through (3). Because of assumption {2}, there is no explicit super-fluid equation. The flow is described in terms of the counterflow speed w, the difference between normal and superfluid velocity. Further, with the second assumption w is approximately equal to the normal fluid velocity. Thus equations (1) to (3) are modified to describe phenomenologically mean field convection quantities:
Continuity

$$\frac{\partial w_x}{\partial x}+\frac{\partial w_y}{\partial y}=0 \tag{A.1}$$

Motion

$$\rho\left\{w_x\frac{\partial w_x}{\partial x}+w_y\frac{\partial w_x}{\partial y}\right\}=-S_L\frac{\partial P_{\text{eff}}}{\partial y}+\eta_n\cdot\frac{\partial^2 w_x}{\partial y^2} \tag{A.2}$$

Excitation system transport

$$\rho w_x \cdot \frac{\partial T}{\partial x} = \eta_n \left(\frac{\partial^2 T}{\partial y^2} \right) \tag{A.3}$$

(η_n normal fluid shear viscosity).

The resulting thermohydrodynamic quantities are analogous to the quantities of He I convection, e.g.

Dominant frequency:

$$f \sim 0.1 (K_\alpha / s)^{1/2} (\Delta T/T)^{1/2} (S_L \, \Delta T)^{1/2} \tag{A.4}$$

Layer thickness:

$$\delta \sim \{ (K_\alpha \, \Delta T/T)(s \eta_n^2)/(\rho^2 S_L^2 \, |\nabla T|) \}^{1/4} \tag{A.5}$$

The ratio $K_\alpha = c_p/S$ is about constant in the range of T with dominant roton excitations. The number of quantized vortices of the cellular pseudo-classical convection is obtained as

$$N_v \sim (s/\Gamma_0) K_\alpha^{1/2} (\Delta T/T)^{1/2} (S_L \, \Delta T)^{1/2} \tag{A.6}$$

Again, a finite number $N_v \to N_0$ at Newtonian fluid convection onset is expected if indeed the excitation system behaves as Newtonian fluid. At present no detailed experimental results appear to be available for an evaluation of N_v.